Available online at www.sciencedirect.com

jmr&t
Journal of Materials Research and Technology

journal homepage: www.elsevier.com/locate/jmrt

Original Article

Regenerated cellulose fabric reinforced bio-based polypropylene sandwich composites: fabrication, mechanical performance and analytical modelling

Pooria Khalili [a,*], *Mikael Skrifvars* [a], *Hom Nath Dhakal* [b], *Chulin Jiang* [b]

[a] *Faculty of Textiles, Engineering and Business (Swedish Centre for Resource Recovery), University of Borås, 510 90, Borås, Sweden*

[b] *Advanced Polymers and Composites (APC), School of Mechanical Design and Engineering, University of Portsmouth, PO1 3DJ, Portsmouth, UK*

ARTICLE INFO

Article history:
Received 16 August 2022
Accepted 29 December 2022
Available online 3 January 2023

Keywords:
Bio-based sandwich composites
Man-made cellulose fabric
Balsa
Mechanical properties

ABSTRACT

Sandwich composites were fabricated successfully with the balsa wood as core material and regenerated cellulose fabric bio-based polypropylene (PP) composite skins. The regenerated cellulose fabric PP composites were produced using two different methods: the conventional stacking lay-up and directly using PP pellets. Sandwich composites were made using the hot press equipment with the customized mold. The sandwich composite system and bio-composite laminate were designed to achieve very close weight to compare the key mechanical properties that each design can bear. It was evidenced from the experimental results that 416% increase in the bending load bearing property of the part can be obtained when sandwich structure was used. These experimental results were in close agreement with one of the analytical modelling utilised. The drop weight impact test results demonstrated that the sandwich specimen is capable of withstanding more than 6 kN load and absorbing the impact energy of 28.37 J.

1. Introduction

Man-made regenerated fibers have been demonstrated to provide substantial promise as reinforcing agents in thermoplastic systems both in the form of short fibers [1,2] and continuous fibers [3]. They offer the merits of both natural and synthetic fibers, which comprise on the one hand low density, CO_2 neutrality, non-abrasiveness to manufacturing equipment and biodegradability of natural fibers (NFs) [4–7], and on the other hand, physical, mechanical and uniform morphological properties of synthetic fibers. Diverse manufacturing routes together with different matrices were experimented to produce rayon (man-made regenerated fiber) thermoplastic systems spanning melt mixing processing followed by injection molding [2,8–10], resin infusion method [3,11] and compression molding for long fiber material systems.

Polypropylene (PP) is a commonly used matrix on account of lowest price and density in comparison with other polymer materials [12] and even other bio-polymers such as polylactic

* Corresponding author.
E-mail address: pooria.khalili@gmail.com (P. Khalili).

https://doi.org/10.1016/j.jmrt.2022.12.186

acid (PLA). Glass fibers (GF) are used as a reinforcement in many applications, however, recent research has been paid special attention to the substitution of GF with NF reinforced PP composites, which possess lower density compared to GF/PP counterparts [12]. These characteristics meet, in particular, the requirements of transport industries where vehicles should be low in weight to decrease fuel consumption and are made of potentially low cost and sturdy materials [13]. Over the last years, the necessity for broadening crude materials and the environmental awareness pursue attempts at use of recourses with renewable nature. Regenerated cellulose fibers offer these merits while inducing good performance. Low density and high tenacity provide high specific strength of resulting PP composites which fit the requirements of light-weight applications. These bio-based composites can be incinerated after utilization [8,10].

The structural properties of regenerated cellulose fabric PP composites can be tailored to reach the desired requirements. For semi-structural applications, sandwich composites are one of the main structures or forms of panels used in industry [14]. Sandwich structures provide low weight and high mechanical properties. Presently, these types of structures are utilised in packaging, automotive, construction and aviation industries among others [15]. These panels consist of two facings bonded to a thick, lightweight core material. Composites and metals are principally used as facings whereas honeycomb structures, foams and balsa wood are the choices of the core material [16]. Employment of NFs in panels is a new research area, and hitherto limited investigations have been performed [17]. Kolahchi et al. [18] studied the buckling of polymeric composite structure containing carbon nanotube (CNT) and carbon fiber for aircraft conical shells and modelled it based on Halpin-Tsai theory, stability performance [19] of magnetostrictive facings loaded with graphene platelets as well as the vibration properties and Young's modulus of polymeric composites consisted of graphene platelets and piezoelectric layers [20].

Different theories can be used to predict the properties of composites: e.g. Mori-Tanaka model was used as the basis to study the effect of earthquake load on concrete pipes reinforced by fiber reinforced composites [21]. In another investigation [22], a method on the basis of Hamilton was selected to obtain the dynamic behaviours of sandwich nanocomposite conical shell in magnetic and thermal conditions. Al-Furjan et al. [23] studied the effective properties of nanocomposite using Halpin-Tsai micromechanics model. The material system was a micro sandwich beam containing core of elastomer.

Replacement of GF with NFs in the sandwich panels was found to enhance the vibration damping and sound properties [24] and to promote significant environmental merits [25] of structures containing thermoset polymers. In another study, synthetic PP polymer and jute fabrics were hot pressed to produce sandwich composites with polyethylene terephthalate (PET) foam, honeycomb PP and balsa core materials [17]. It was found out that the flexural rigidity increased outstandingly as compared to that of composites without the core. It was also revealed that laminates with the balsa wood core demonstrate greater bending rigidity than the panels with other cores used in this investigation. Some models are used to predict the mechanical performance of the composite structures. For instance, sandwich composites filled with graphene platelets were modelled based on the Halpin-Tsai micromechanics theory to obtain Young's modulus [26]. Several methods of tensile test studies for fiber reinforced polymeric composites were reported in Al-Furjan et al. article [27].

Very few works have been reported on utilization of regenerated cellulose fabrics in sandwich panels. Moreover, to the best of authors' knowledge, utilization of bio-based PP in sustainable sandwich bio-composites has not been investigated prior. The combination of the regenerated cellulose fabric (rayon in this study) and the bio-based PP were not considered for composite production as either composites or facing materials used in panels thus far. In this work, the above-mentioned composite laminate and bio-based sandwich composites were manufactured. The PP polymer used had about 30% bio content and labelled as recyclable like other synthetic PPs. It is specified as a grade of high impact resistance, good processability and medium stiffness. This PP grade is processed similar to other synthetic PP types in order to make parts. The effect of incorporation of rayon fabrics in the bio-based PP in terms of tensile and flexural properties was investigated. The impact of inclusion of the polymer in the forms of pellets and films on the mechanical properties of the composites were also studied. The bending behavior of sandwich bio-based composite, balsa wood and the control composite were focused, and the flexure of sandwich panel was modelled with Euler-Bernoulli and Timoshenko theories. Additionally, the load bearing capability and energy absorption performance of sandwich structure under low velocity impact test was also investigated, which were not focused much on previous experiments before with these constituents included in the composite skins.

2. Materials and methods

2.1. Materials

The bio-based PP containing around 30% bio-based content was purchased from NaturePlast, France. PP possessed the density (23 °C) and melt flow index (230 °C) of 0.9 g/cm^3 and 70 g/10min, respectively. 0/90 man-made cellulose (rayon) fabrics were provided by Cordenka company, Germany. The Cordenka® 700 2440 dtex had an areal weight and density of 442 g/m^2 and 2482 dtex, respectively. Balsa wood used as core material in the sandwich composite was purchased from hobbymodeller, Sweden, and had the density and thickness of 0.12 g/cm^3 and 6 mm, respectively. Rayon fabrics were dried in a convection oven for a period of 24 h at 70 °C prior to the composite processing to avoid moisture absorption. PP films and pellets were also dried for the same time at 40 °C before further processing.

2.2. Film preparation and optimization

PP granules were compressed into films with the aid of a 20-ton manual bench press equipment (Rondol Technology Ltd., UK). The area, where granules was pressed, was measured 190 mm (length) × 190 mm (width) and it was aimed to obtain

around 0.4 mm thick bio-based PP films. To achieve the target thickness, varying compressive pressure and amounts of PP pellets were used for a period of 60 s at 200 °C. Ultimately, 0.8 bar pressure was applied to 10 g bio-based PP in order to attain the 0.4 mm thick film. This resulted in the target fiber mass fraction in the composite by optimizing the PP film thickness obtained by varying press pressure and PP quantity. Fig. 1 illustrates the various process parameters used for optimization of PP film thickness.

2.3. *Rayan PP composite and sandwich manufacturing*

A conventional film-stacking method, constructed by the addition of alternating layers of man-made cellulose fabric and PP film, was used to produce rayon fabric PP-sheet composites using the same hydraulic hot press utilised for the film fabrication. After stacking the layers as per Fig. 2 (which included three layers of rayon (R) and five sheets of PP film) in the 2 mm thick mold, the press pressure was gradually increased in 1 min to reach the level of 50 bar (5 MPa) at 200 °C. Then, the whole system was held for a period of 10 min for consolidation before cooling the material under 0.08 bar pressure for 180 min at room temperature (RT). The composite plates measuring 180 × 180 × 2 mm with the fiber mass fraction of 61.4 wt% was obtained from this manufacturing system.

A composite laminate production method with the aid of PP pellets was also performed for comparison purpose. PP pellets were manually distributed between the three layers of the rayon fabrics in the same 2 mm thick mold. The weight of fiber was subtracted from the mass of rayon reinforced PP film composite to use the same amount of PP for the composite fabricated with the direct use of PP pellets. The final mass of rayon reinforced PP pellet-based composite was then weighed to ensure that the same weight for both types of the composites was obtained. Exactly, the same fabrication conditions as described above were applied. The whole material system underwent

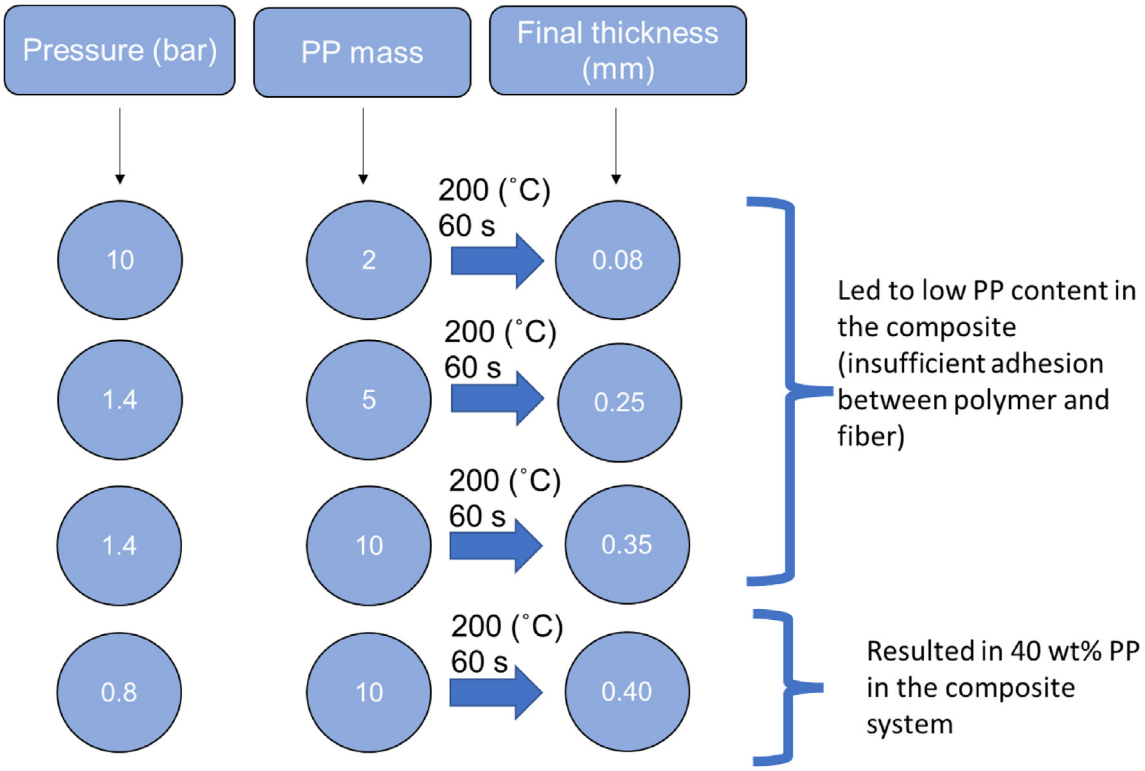

Fig. 1 – The method of optimization for PP film to obtain the required thickness.

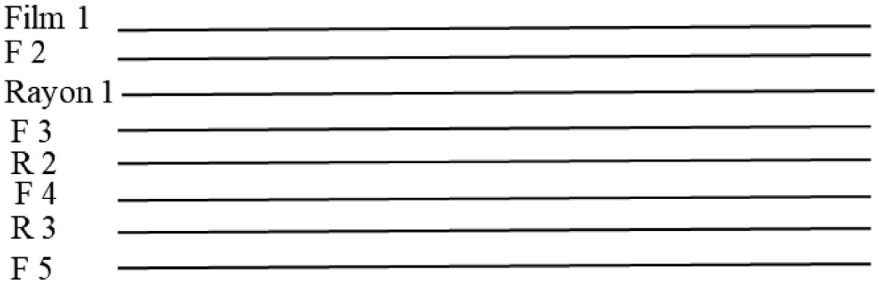

Fig. 2 – Composite laminate design.

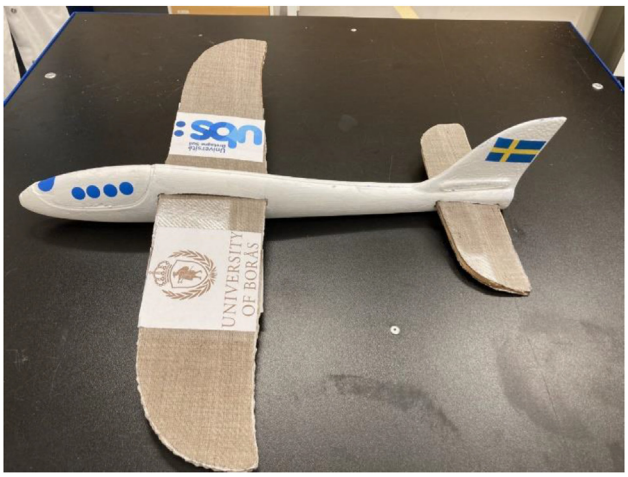

Fig. 3 – Flying wind demonstrator with wings and tails made of bio-based sandwich composite with the balsa wood core.

continuous pressure in 1 min to reach 5 MPa pressure at 200 °C. The assembly was under the pressure for 10 min and subsequently, was cooled down with the same above-mentioned condition at the RT. In the same manner, neat bio-based PP polymer plate was also prepared with 100 wt% of the polymer as the control, measuring 2 mm thickness. It is worth mentioning that the wings and tails of a flying plane (toy), which was originally made from foam polymer, were successfully replaced with bio-based PP composites containing the balsa core as a demonstrator (Fig. 3).

The rayon bio-based PP sandwich composite with the balsa wood core was fabricated in such a way that a layer of rayon fabric was placed at the top and another one at the bottom of balsa wood. On top and bottom of each viscose fabric a layer of PP sheet was positioned and the whole assembly was placed in a mold measuring the cavity of 100 × 100 × 7 mm (Fig. 4). A layer of PTFE film was placed on the very top and bottom surface of the assembly for easy demolding. Ultimately, a bio-based sandwich composite with balsa as core material was produced and the resulting composite panel had the thickness of 7 mm. In order not to create permanent deformation to balsa wood while compacting, the whole sandwich composite was hot pressed for the same duration, 10 min, as rayon fabric PP sheet composite laminate was produced, at 0.5 MPa pressure (which was lower than the compressive strength of the balsa wood). The bending test samples were cut along the axial grain direction of the balsa wood using the laser cutting machine. Scanning electron microscope (SEM) tests were performed on the fractured bio-based panel and the balsa wood core.

3. Characterizations

The neat PP, bio-based composite laminate and sandwich composite samples were tested under bending loading according to BS EN ISO 14125 [28] with the aid of a Tinius Olsen H10KT universal testing instrument and their flexural properties were compared. The crosshead speed of 5 mm/min, span length of 64 mm and sample dimension of 80 mm (length) × 20 mm (width) were used for the tests. The load-cell of 250 N was connected to the equipment. All the specimens were conditioned for 24 h at the humidity of 50% and the temperature of 23 °C prior to the testing. The average values of the results were accordingly reported.

The tensile behaviors of dog-bone man-made cellulose fabric composite and neat PP polymer samples were investigated in accordance with EN ISO 527-4 (type 1B specimen) [29]. The crosshead speed of 2 mm/min, initial distance between the grips of 115 mm and span length of 50 mm was used for the tests. The equipment was connected to the load-cell of 5 kN and the instrument was equipped with a 100R mechanical extensometer. A GCC Laserpro Spirit GLS instrument was

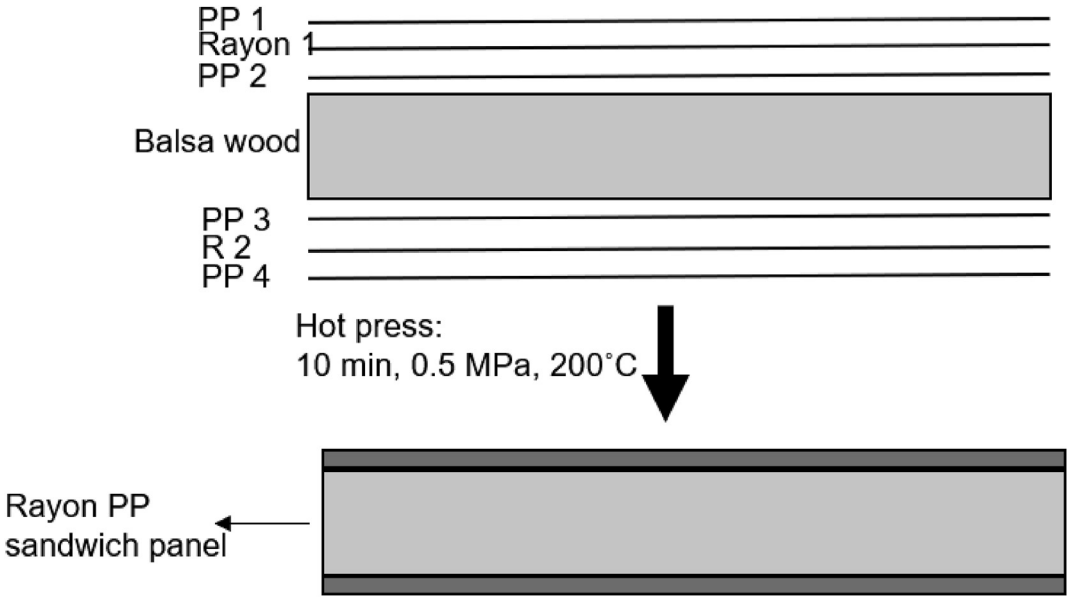

Fig. 4 – Schematic diagram of the sandwich composite preparation.

used for all the composite sample preparations. The samples were conditioned for 24 h at the temperature of 23 °C and the humidity of 50% prior to the testing.

The low velocity impact tests were performed on the sandwich composite and the balsa wood specimens using a Zwick/Roell HIT230F drop weight tester. Three sample dimensions measuring 70 × 70 mm were cut by a laser cutting instrument (GCC Laserpro Spirit GLS, Borås, Sweden). The weight of impactor was 23.11 kg, which includes both impactor mass of 22.832 kg and tup mass of 0.278 kg. This creates a 25-J incident energy by falling the impactor from the height of 110 mm at the ambient temperature. The diameter of the tup, which is made of the hemispherical steel, was 19.8 mm. The samples were mounted on the rigid clamping supports. With the aid of a strain-gauge striker and a load-cell installed on the machine several parameters were obtained. Displacement, force, time and absorbed energy were recorded during the tests. In order to prevent multiple impacts on the samples, an anti-rebound device was connected to the instrument.

SEM test was performed on the fractured sandwich biocomposite and balsa wood samples after the impact test to obtain the SEM micrographs. A Philips XL30CP SEM instrument was used to scan the impacted sandwich composites. The samples were first prepared by metallizing with a thin gold layer in a vacuum condition, and subsequently were scanned at a 15 kV voltage. The sandwich specimens after the bending and low velocity impact tests were found to have no debonding or delamination between the core and the skins. Therefore, the specimen after the impact test was chosen, and the composite skin was scanned at the cross-section, where a separation between the fracture part and the whole specimen was formed, to investigate the microstructure of the composite skin after the fracture.

Digital imaging microscope tests were carried out to investigate the interfacial adhesion between the core and the composite skin in the sandwich panel and between the fabric layers and the bio-based PP polymer in the rayon PP sheet composite sample after the processing. An eclipse LV150 N microscope-digital imaging combined with advanced optical system was used to capture the cross-sectional images of the samples without surface coating.

Differential Scanning Calorimetry (DSC) tests were performed on only the PPs selected from three different formulations, namely neat PP, rayon PP pellet and rayon PP film. This was to evaluate the crystallinity levels and melting behavior of the PP for these three formulations due to varying processing of PP in these material systems. A DSC-2000 apparatus (TA Instruments, USA) was used to test the samples. Samples weighing 5–10 mg were placed in covered aluminum crucibles. The samples were heated from −40 to 200 °C at a ramping rate of 10 °C/min in nitrogen atmosphere and the flow rate of nitrogen gas was set to 50 mL/min. Samples were maintained for 2 min at 200 °C to avoid the inclusion of the thermal history in the measurements. Then, the samples were cooled down to −40 °C at the same heating rate. The samples were kept for 2 min at −40 °C and subsequently were heated up to 200 °C at 10 °C/min heating rate. The measurements reported were from the second and third cycles of the tests.

4. Results

4.1. *Bending properties of composites*

The bending strength and modulus values of neat bio-based PP, man-made cellulose fabric PP sheet composites and man-made cellulose pellet composite laminates are displayed in Table 1. The bending strength and modulus were 22.8 MPa and 0.97 GPa for the control, respectively. The combination of rayon fabric and PP sheet to make the composite led to significant improvement in modulus (2.71 GPa) by 180% increase. The strength was found to enhance by 13% as well. This demonstrates the reinforcing effect of bio-based fabrics in the composite. Using PP in the form of pellets in the composites was seen to enhance the flexural performance as compared to that of neat PP whereas the flexural strength and strain were found to decrease in comparison with those of rayon PP sheet composite laminate counterpart. This implies that PP sheets provide better distribution of PP in the fabric layers. Ganster et al. [8] investigated the bending properties of rayon tyre cord yarn reinforced PP composite for injection molding applications. The flexural modulus was obtained approximately 2.60 GPa at the fiber weight fraction of ca. 40% in this study. Karaduman et al. [17] produced 15 wt% jute reinforced synthetic PP composite using the hot press equipment and the stiffness obtained was 1.88 GPa whereas the neat synthetic PP demonstrated the modulus of 1.20 GPa. These values prove the practicality of rayon bio-based PP composite systems with a high percentage of the bio content in terms of the mechanical behaviors.

The samples were examined after the tests, and it was found out that the neat PP and composite laminate samples did not break, and the mode of fracture was micro-cracks on their compression (top) sides. No sign of delimitation was also observed in the samples.

The intrinsic mechanisms of a sandwich panel are to provide a high stiffness (/weight ratio) as compared to material systems without core. A thicker core possessing less stiffness and strength than facings is bonded to two skins with stronger and stiffer properties. The material system promotes enhanced flexural performance with the incorporation of low density, thick and soft core whilst ensuring a panel of lightweight structure [14]. Sandwich composite samples with 6 mm thick balsa wood core were tested to compare with the rayon reinforced bio-based PP composite laminate specimens measuring 2 mm thickness. The sandwich composite was designed in such a way to have proximately the same weight as the composite laminate, as seen in the weight ratios in Table 2. The deflection-force curves of the sandwich composite, rayon PP

Table 1 – Flexural properties of bio-based PP and rayon composites.

Samples	Strength (MPa)	Strength SD (MPa)	Modulus (GPa)	Modulus SD (GPa)
Neat PP	22.80	0.50	0.97	0.01
Rayon PP sheet	25.80	0.90	2.71	0.10
Rayon PP pellet	23.48	0.60	2.42	0.10

Table 2 – Comparison between the bio-based composite skin and its respective sandwich structure, as obtained from the bending test results and flexural test specimens.

Samples	Bio-composite skin	Sandwich composite along the wood grain direction	Balsa wood
Thickness (mm)	2	6.8	6
Weight (g)	3.22	3.4	0.62
Weight ratio	1	~1.05	–
Max. Force	20.8	107.3	45.8
Initial slope ratio	1	14	4.5

laminate and balsa wood are shown in Fig. 5. The bio-composite skin was found to offer approximately 21 N whereas the greatest force was recorded for the sandwich composite with the value of 107.3 N at the deflection of approximately 2.1 mm demonstrating 416% increase in load-bearing potential of the part. This demonstrates the successful production and excellent effectiveness of the sandwich composites. Balsa wood was seen to reveal higher maximum force capacity (~46 N) than that of the composite laminate. It is known that man-made cellulose fibers show lower stiffness than NFs [3,30], and the incorporation of the core material can compensate significantly for this issue.

The force-displacement behaviors of all three types of materials were totally different and presented varying trends (Fig. 5). The composite skin was seen to demonstrate an elastic-plastic deformation with a high value of elongation to break. Balsa wood tested along the grain direction was found to show greater stiffness than that of the bio-composite laminate along with a more kind of the elastic behavior. However, the sandwich bio-composite can be seen that proving a totally different behavior than the other two types of materials. The elastic slope of the sandwich composite was 14 times faster than that

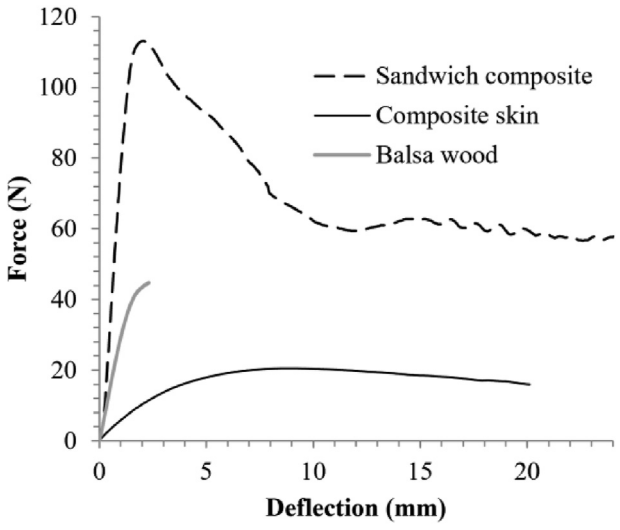

Fig. 5 – Comparison of force-deflection responses between sandwich composite, balsa wood and composite skin.

of the bio-based composite skin, which confirms again the great effectiveness of the sandwich composite for nearly the same weight as composite laminate. The sandwich composite provided a synergy in such a way that possesses enhanced properties in terms of force-displacement and ultimate load bearing capacity. Moreover, the displacement followed the trend of the bio-composite laminate i.e. a very long deflection.

Fig. 6 illustrates the top and bottom surfaces of the balsa wood samples after the flexure. It can be observed that the material bent under the load and dented on the top surface (Fig. 6 (a)). At the bottom of the specimens, a continuous crack along the width, right below where the load was applied, was observed. For the bio-based sandwich structures with the balsa wood core, the upper composite skin and the core, as shown in Fig. 7 (a) and (b), were compressed and depicted a dent, respectively. The lower surface of the bio-based composite, however, experienced some micro cracks along the width of the specimens at the tension side of the panel (Fig. 7 (c)). It is important to note that no sign of delamination was detected for the sandwich composites with the balsa core in this work, however, as investigated in another study, in case of PET foam and PP honeycomb based sandwiches with jute fabric composite skins, the panels experienced a significant delimitation under flexure [17]. Moreover, they stated that Balsa sandwich provided greater flexural performance than that of PET foam core and the PP honeycomb core sandwich bio-composites.

4.1.1. *Modelling the bending properties of balsa wood sandwich bio-composites:*

In order to predict the force-deflection behavior of sandwich composites the panel was modelled using both Euler-Bernoulli and Timoshenko beam theories, and the estimations of models were compared with the flexural test results. The boundary conditions were based on the two fixed supports with the span length of 64 mm where the sample was resting on and a load applied to the middle of the specimen allowing the displacement in -Y direction. According to Euler-Bernoulli beam theory, the differential equation of the displacement curve for beams loaded transversely is [31]:

$$EI\frac{d^2y}{dx^2} = -M \tag{1}$$

where M is the flexural moment, I is defined as the moment of inertia of the cross-section (with regard to the neutral axis), and E is the elastic stiffness.

In the event of three-point bending force, the ultimate displacement (y_{max}) obtains in the middle of the beam as follows:

$$y_{max} = \frac{Pl^3}{48EI} \tag{2}$$

where P is the bending force, l is the flexural span length, and EI is the bending rigidity, which, for the materials with core, can be obtained based on the equation below [32]:

$$EI = E_f\frac{btd^2}{2} \tag{3}$$

where E_f is the tensile modulus of the skin, b is the width of the sandwich material, t is the thickness of each skin layer, and d is the distance between the central axes of the two facings.

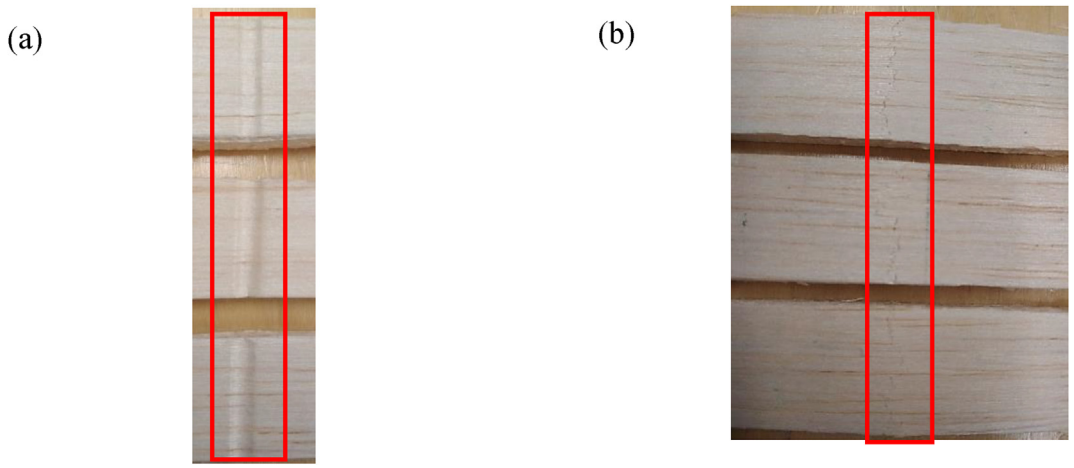

Fig. 6 – (a) The middle view of the top balsa wood samples and (b) the middle view of the bottom surface of the balsa wood samples after bending.

The maximum displacement at the middle of the beam (y_{max}) is obtained with the equation below:

$$y_{max} = \frac{Pl^3}{24E_f btd^2} \tag{4}$$

The equation (4) (Euler-Bernouli) neglects the impact of shear, however Timoshenko model considers additional displacement as a result of shear forces. Therefore, the maximum displacement at the middle of the sandwich beam in three-point bending scenario is:

$$y_{max} = \frac{Pl^3}{48EI} + \frac{\alpha}{AG}\frac{Pl}{4} \tag{5}$$

where A is the cross-sectional area and calculated as $A = bd^2/c$ for sandwich composites (c is the core thickness), α is the shear correction factor and G is core shear modulus.

The two terms in equation (5) demonstrate the displacement under flexure and additional deflection owing to shear forces, respectively. On the condition that sandwich composite is comprised of two composite skins (facings), Birman and Bert [33] recommended taking α equal to 1. Hence, the maximum displacement at the middle of the sandwich structure for three-point bending can be obtained using the equation as follows:

$$y_{max} = \frac{Pl^3}{48EI} + \frac{Pl}{4AG} \tag{6}$$

In order to determine the sandwich beam shear properties and calculate the core shear modulus, the following three equations (7)–(9) were used according to ASTM D:7250/D7250 M – 06 [34]. The equations are valid if the facings are identical, and a single loading configuration test is carried out.

$$D = \frac{E_f\left(d^3 - c^3\right)b}{12} \tag{7}$$

$$U = \frac{P(S-L)}{4\left[\Delta - \frac{P\left(2S-3SL^2+L^3\right)}{96D}\right]} \tag{8}$$

$$G = \frac{U(d-2t)}{(d-t)^2 b} \tag{9}$$

where D is flexural stiffness ($N.mm^2$), U is transverse shear rigidity, S is support span length (mm), L is the load span length which is 0 for three-point mid-span configuration), Δ is the beam mid-span deflection (mm) and G is core shear modulus (MPa).

Bending force vs. deflection curves of sandwich bio-composite obtained from the experiment, Euler-Bernoulli

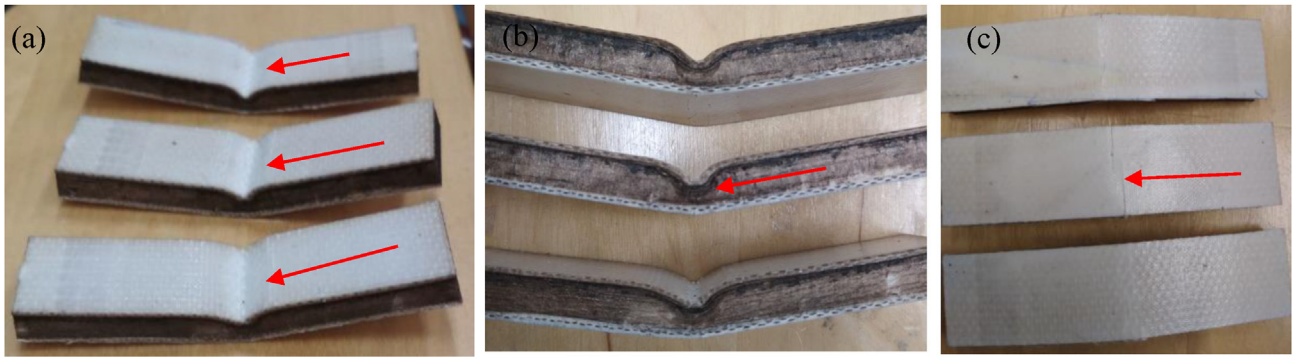

Fig. 7 – The images of the sandwich composites after the flexure: (a) the upper composite skin bent, (b) the core material bent together with the upper skin and (c) the bottom bio-based composite skin.

model and Timoshenko model are presented in Fig. 8. The prediction from Euler-Bernouli model was found to underestimate the deflection of the sandwich structure, which is ascribed by the neglection of the displacement occurred by the shear effect. This model provides inaccurate estimation when the core shear modulus is low as the core material is the primary element which bears the shear loads [17]. However, when deflection caused by shear loads were taken into account (Timoshenko model), the model gave greater prediction with the experimental flexure in the elastic phase of the curve. This emphasizes that shear forces cannot be disregarded for this sort of sandwich structures. Similarly, it was reported that for paper reinforced epoxy sandwich composites with aramid honeycomb core [35] and for jute fiber reinforced composite structure with PP honeycomb core [17], Timoshenko model provided good agreements with the experiment that the Euler-Bernoulli theory. Timoshenko model is even more prominent and provides better agreement with the experiment when no significant amount of delamination occurs under the flexural loading, which was the case for our composite panel.

4.2. *Tensile behavior of composites*

Tensile test was also carried out to investigate the effect of the addition of the regenerated man-made cellulose fabrics into the bio-based PP and the influence of incorporation of the PP in the form of pellets in the composites. It was revealed that the rayon fabric PP-sheet composite substantially enhanced the tensile properties as compared to those of neat bio-based PP, and it demonstrates the reinforcing effect of man-made cellulose fabrics. For the tensile strength, the values increased from 20 MPa to 98 MPa, proving 390% improvement (Table 3). The Young's modulus was seen to improve from 1.12 GPa to 3.1 GPa showing nearly 177% enhancement. These results can be ascribed to the superior tensile performance of the rayon fabrics. The reinforcing effect was also significant on the ductility of the composite, and the inclusion of rayon

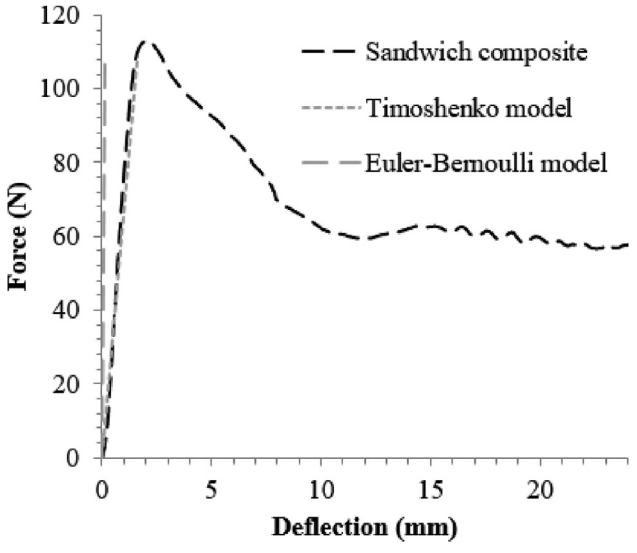

Fig. 8 – Force-deflection behavior of sandwich composite as obtained from the experiment and models.

Table 3 – Tensile properties of the bio-based PP and rayon composites.

Samples	strength (MPa)	elongation to break %	modulus (GPa)
rayon pp pellet	93	30	2.5
rayon pp sheet	98	32	3.1
PP	~20	~6	1.12

fabrics into the PP polymer was found to considerably increase the elongation to break from 6% to 32%.

However, the combination of PP pellets and rayon fabrics could not reach the level of tensile properties of those of rayon PP film composite counterpart. When the bio-based PP was utilised in the form of pellet to make the rayon fiber PP composites, all tensile properties showed an apparent decrease in particular modulus relative to those of rayon fiber composite made of the PP sheets. The modulus, strength and elongation to break were recorded 2.5 GPa, 93 MPa and 30%. This demonstrated the importance of uniform thermoplastic distribution and impregnation throughout the fabrics.

Johonson et al. [1] studied the tensile strength and modulus of wetlaid lyocell PP composites produced using a hot press, and the tensile strength reported was 29% lower than that of rayon PP sheet composites investigated in the current study at the same fiber mass fraction whereas nearly the same modulus was recorded for the lyocell PP composite and rayon reinforced bio-based PP composite counterpart. The difference between the elongation break values were substantial, and the value of rayon PP composite from this study was found to be 75% higher that of wetlaid lyocell PP composite.

4.3. *Impact test analysis*

4.3.1. *Force-displacement behaviors*

Displacement versus force curves obtained from the drop test for sandwich bio-composite and balsa wood samples are depicted in Fig. 9.

From the curves of the sandwich composite specimens, stable propagation of the force with respective to the displacement can be found. The average maximum force was recorded 6051.53 N at the depth of 7 mm (Table 4) whereas the force-displacement behavior was different for the balsa wood specimens. The force had sort of unstable trend indicating the weight penetration in the specimen, fracture and tear as illustrated in Fig. 10. Without the presence of composite skins, it was observed that the balsa wood core demonstrated a very small maximum force of 75.98 N at the depth of approximately 2.25 mm as compared to that of the sandwich bio-composite. The maximum force was recorded almost 80 times higher for the sandwich composite specimens.

The images (Fig. 10) illustrate that unlike wooden samples, which failed completely, and the incident energy penetrated the wood, the sandwich composite specimens were observed to perforate significantly lesser (Fig. 10) (c) and (d). This could be concluded that sandwich composites resist failure by dissipating and absorbing energy.

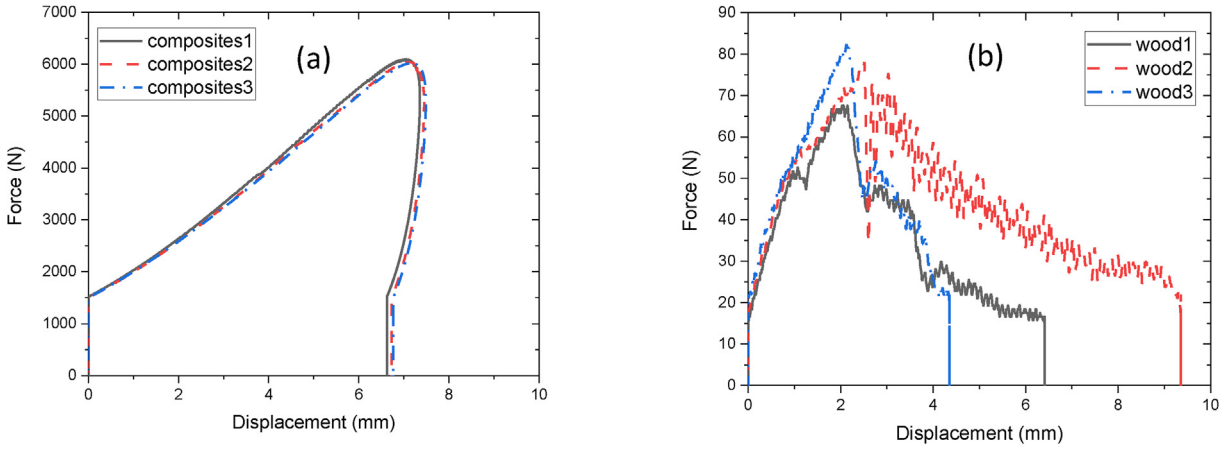

Fig. 9 – Force-displacement curves for (a) sandwich composite and (b) balsa wood specimens.

4.3.2. *Force-time behaviors*

The force-time results corresponding to the impact scenario for both balsa wood and sandwich bio-composites are shown in Fig. 11 (a) and (b). The force plotted is reaction force exerted by the samples to the impactor tup. The sandwich composites were seen to demonstrate a mountain-like trend similar to parabolic whereas the force-time behavior was different for the balsa wood. A very sharp increase to the ultimate force was observed after around 23 ms contact with the impactor, followed by a prompt load drop due to easy fracture of balsa wood grains, however, it took approximately 35 ms for the sandwich specimens to reach the maximum force. This proves the significant improvement of impact resistance in the sandwich composites, and that the initial damage and fracture occurred over a longer period.

4.3.3. *Energy-time behaviors*

The absorbed energy-time curves are depicted for the sandwich composite and the balsa wood specimens. It was revealed that the enhancement of impact energy was substantial with the incorporation of the bio-based composite skins (Fig. 12 (a) and (b)). It was found that the maximum energy improved by 98 times when the sandwich composites were tested. The balsa wood specimens were entirely penetrated (Fig. 10 (a) and (b)), allowing the energy to pass through the balsa wood, and therefore, a small amount of energy (0.29 J) was absorbed. However, upon the incident energy of 25 J, the sandwich composite specimens did not puncture, and the maximum energy was recorded 28.37 J for the sandwich bio-composites.

Table 4 – Average drop test results for the wood and sandwich composites.

Specimens	Average Maximum Energy (J)	SD (J)	Average Maximum Force (N)	SD (N)
Wood	0.29	0.11	75.98	7.6
Sandwich Composite	28.37	0.07	6051.5	30.71

4.3.4. *Failure and damage modes*

Post-impact visual inspection for the balsa wood and sandwich composite are illustrated in Fig. 10. The balsa wood images (Fig. 10 (a) and (b)) present the damage to the wood specimens and full penetration of the impactor as a circular shape chunk was cut out from the samples. For the sandwich composite specimens (Fig. 10 (c) and (d)), some cracks are visible. On the front side of the sandwich specimen, a small round crack formed whereas matrix cracking occurred mainly in the middle of the specimen on the rear side.

4.3.5. *Scanning electron microscope (SEM) of fractured surface of the sandwich composite and balsa wood specimens*

Fig. 13 shows SEM images of the sandwich structure and balsa wood after fracture. Fig. 13 (a) illustrates the cross-sectional image of the composite facing after the impact test and its separation from the sandwich composite. It can be observed that the fiber breakages, matrix cracking and slight delamination are clear in the facing and are predominant failure modes. For the balsa wood image, as shown in Fig. 13 (b), the cross-sectional view of the structure of the balsa wood (the axial grain direction) shows kind of honeycomb pattern of the cells, which could also contribute to the load absorption capacity of resulting sandwich composites.

4.4. *Digital imaging analysis*

Fig. 14 presents the microstructure of the sandwich composite with the PA core material and the facing as well as the rayon PP sheet composite. As observed in Fig. 14 (a), good interfacial adhesion between the core and the facing can be observed, as highlighted in the red rectangular. Fig. 14 (b) illustrates sufficient bonding between the fabric and PP polymer in the cross-sectional view.

4.5. *Crystallization and melting behaviours*

The DSC thermograms of PP samples in neat PP and composites with the incorporation of PP pellets and PP films are depicted in Fig. 15. The crystallization temperature T_c (°C), melting temperature T_m (°C), crystallization enthalpy ΔH_c (J/g),

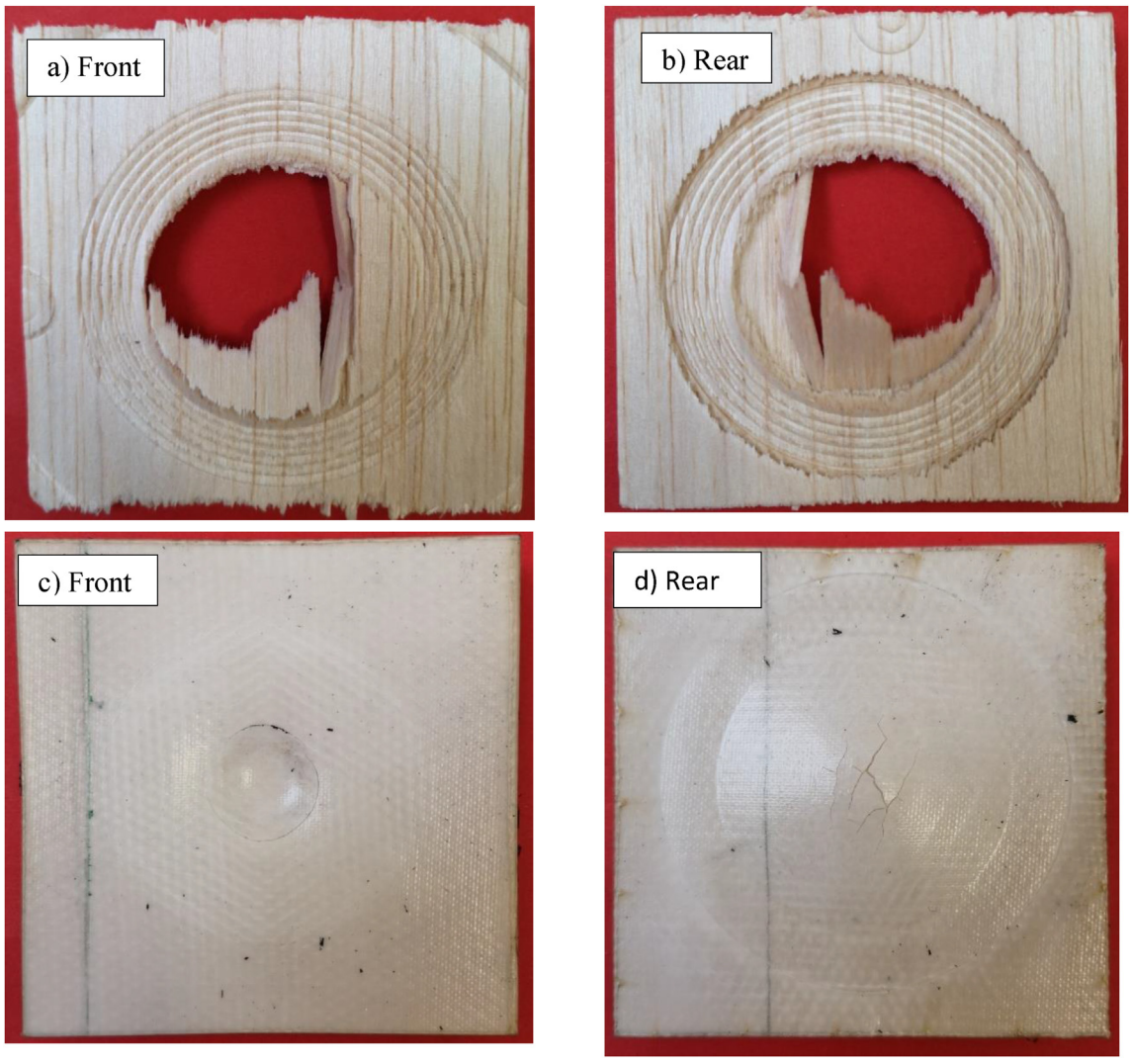

Fig. 10 – Visual images demonstrating damage patterns of the specimens: (a) wood (front face), (b) wood (rear face), (c) sandwich composite (front face) and (d) sandwich composite (rear face) after the drop test.

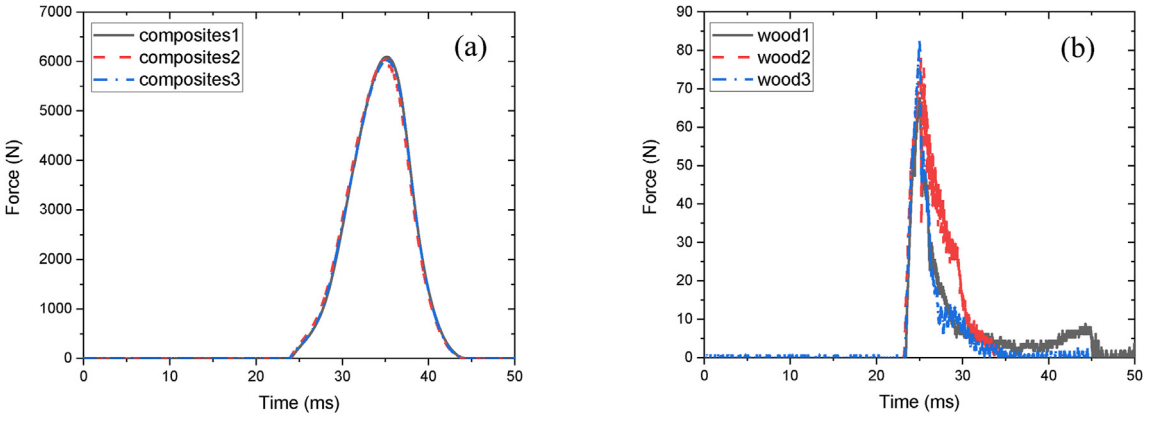

Fig. 11 – Force versus time curves of the sandwich specimens and balsa wood samples.

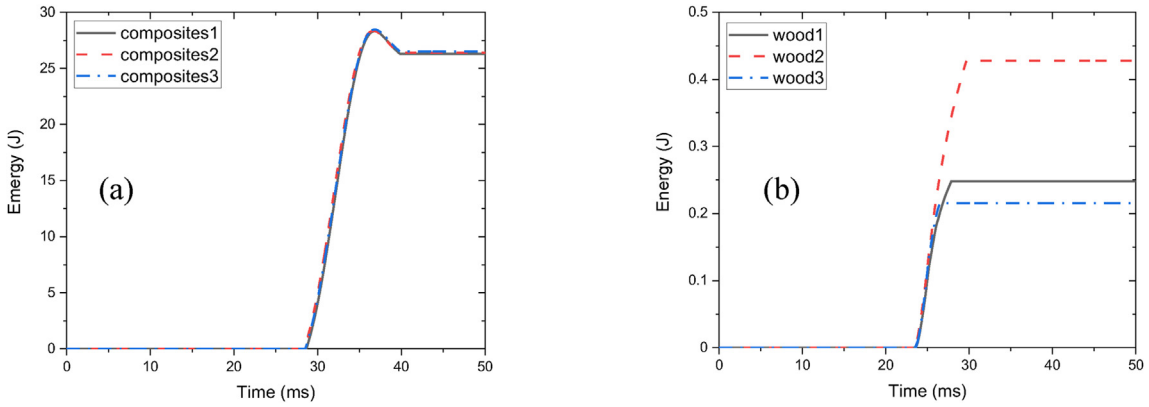

Fig. 12 – Energy vs. time for (a) the sandwich composite and (b) the balsa wood samples.

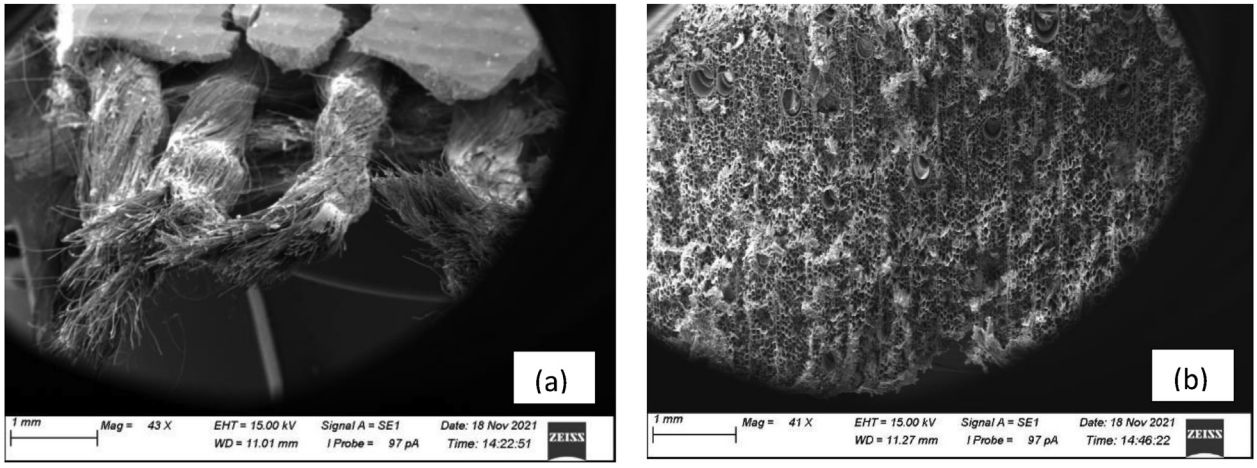

Fig. 13 – SEM micrographs of (a) the sandwich composite and (b) balsa wood after the impact test.

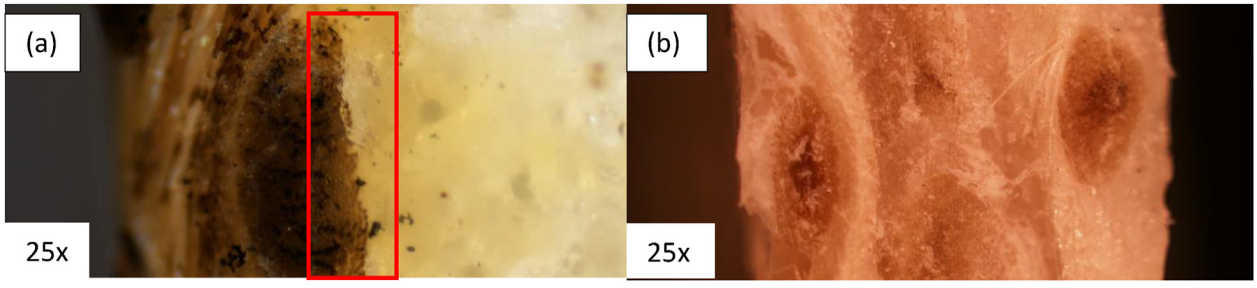

Fig. 14 – Microscopy images of the interface (a) between the composite skin and PA textile core and (b) between the fibers and bio-based PP at 25× magnification.

melting enthalpy ΔH_m (J/g) and degree of crystallinity X_{DSC} (%) are measured and displayed in Table 5. Almost no change was found to detect in all the above-mentioned parameters where the PP was used in the forms of either pellets or sheets in neat PP, rayon PP pellet and rayon PP film. T_c and T_m were obtained around 121–122 °C and 162–163 °C, respectively. For the calculation of the degree of crystallinity, the heat of fusion of pure crystalline PP, ΔH_0, was taken as 209 J/g [36,37], and the value of the degree of crystallinity was calculated ca. 36–37%. This demonstrates that the intrinsic thermal behaviours of the polymer system did not alter with the inclusion of the PP in either form in the neat PP and composites.

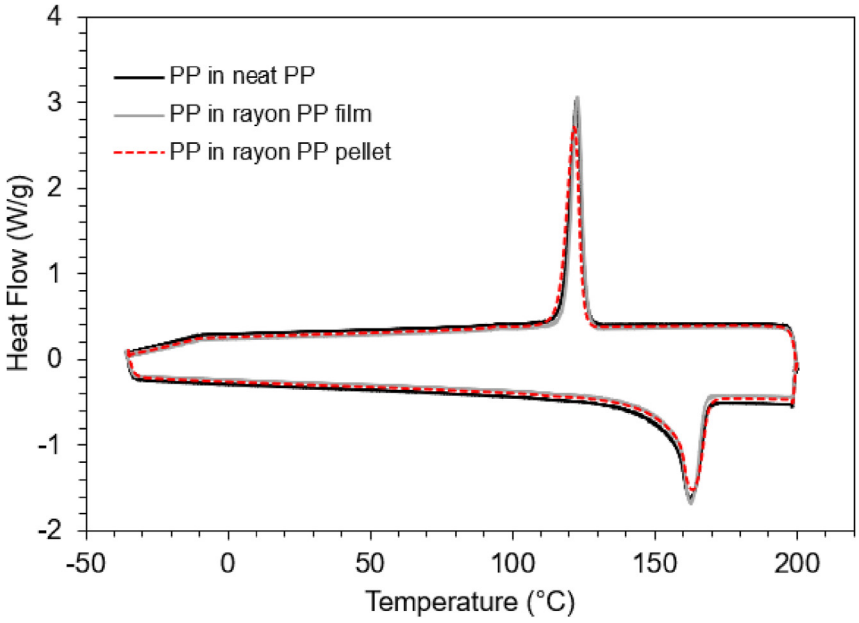

Fig. 15 – Differential scanning calorimetry (DSC) thermograms of PP in neat PP, rayon PP film and rayon PP pellet.

Table 5 – The T_c, T_m, ΔH_c, ΔH_m and X_{DSC} obtained from the DSC measurements for PP in neat PP, rayon PP film and rayon PP pellet.

Samples	T_c (°C)	T_m (°C)	ΔH_c (J/g)	ΔH_m (J/g)	X_{DSC} (%)
Neat PP (in PP plate)	122.5	162.6	84.8	79.1	37.8
PP in the composite in the form of pellets	121.6	163.3	84.2	77.0	36.8
PP in the composite with PP films	122.7	162.8	82.8	76.8	36.7

5. Conclusions

The experimental work was designed to study the effect of bio-composite design on the mechanical performance of the composites and the bio-based sandwich composite. The effect of regenerated cellulose fabrics as reinforcement was significant in terms of the improvement of tensile properties and bending modulus as compared to those of neat bio-based PP. The enhancement of flexural properties for both maximum force and initial slope of elastic region was remarkable when balsa core material was used to make sandwich composite system without tangible weight increase. Under the flexure, the sandwich bio-composite samples did not present any evidence of delamination. The bending force-displacement of the sandwich specimens were predicted using the Euler-Bernoulli and Timoshenko models, which the latter theory provides more precise estimation due to the consideration of shear forces in the concept. With the incorporation of the thin regenerated cellulose fibre reinforced bio-based PP composite facings onto the balsa core, the energy absorption and ultimate force of sandwich composites was found to record significantly higher values than the wood after the low velocity drop test. Besides, SEM test analysis was carried out to detect the mode of impact test fracture which was mainly the fiber breakages and matrix cracking. For the future work, it is suggested that film extrusion equipment can be used to provide a more precise and faster solution for the thermoplastic film making process.

Declaration of competing interest

The authors declare that they have no known competing financial interests or personal relationships that could have appeared to influence the work reported in this paper.

Acknowledgments

This research was funded by ÅForsk foundation, grant number 20-412 and knowledge foundation (KK-stiftelsens) fund number 20200142. Special thanks to Cordenka for sponsoring the rayon fabrics.

REFERENCES

[1] Johnson RK, Zink-Sharp A, Renneckar SH, Glasser WG. Mechanical properties of wetlaid lyocell and hybrid fiber-

reinforced composites with polypropylene. Compos Appl Sci Manuf 2008;39(3):470–7.
[2] Franciszczak P, Merijs-Meri R, Kalniņš K, Błędzki AK, Zicans J. Short-fibre hybrid polypropylene composites reinforced with PET and Rayon fibres – effects of SSP and interphase tailoring. Compos Struct 2017;181:121–37.
[3] Khalili P, Skrifvars M, Ertürk AS. Fabrication, mechanical testing and structural simulation of regenerated cellulose fabric Elium® thermoplastic composite system. Polymers 2021;13(17):2969.
[4] Khalili P, Blinzler B, Kádár R, Blomqvist P, Sandinge A, Bisschop R, et al. Ramie fabric Elium® composites with flame retardant coating: flammability, smoke, viscoelastic and mechanical properties. Compos Appl Sci Manuf 2020;137:105986.
[5] Khalili P, Tshai KY, Kong I. Natural fiber reinforced expandable graphite filled composites: evaluation of the flame retardancy, thermal and mechanical performances. Compos Appl Sci Manuf 2017;100:194–205.
[6] Alhijazi M, Safaei B, Zeeshan Q, Asmael M, Eyvazian A, Qin Z. Recent developments in Luffa natural fiber composites: review. Sustainability 2020;12(18):7683.
[7] Mohamad A, Qasim Z, Zhaoye Q, Babak S, Mohammed A. Finite element analysis of natural fibers composites: a review. Nanotechnol Rev 2020;9(1):853–75.
[8] Ganster J, Fink HP, Pinnow M. High-tenacity man-made cellulose fibre reinforced thermoplastics – injection moulding compounds with polypropylene and alternative matrices. Compos Appl Sci Manuf 2006;37(10):1796–804.
[9] Ganster J, Erdmann J, Fink HP. Biobased composites. Polimery 2013;58(6):423–34.
[10] Franciszczak P, Bledzki AK. Tailoring of dual-interface in high tenacity PP composites – toughening with positive hybrid effect. Compos Appl Sci Manuf 2016;83:185–92.
[11] Khalili P, Kádár R, Skrifvars M, Blinzler B. Impregnation behaviour of regenerated cellulose fabric Elium® composite: experiment, simulation and analytical solution. J Mater Res Technol 2021;10:66–73.
[12] Karian H. Handbook of polypropylene and polypropylene composites, revised and expanded. CRC press; 2003.
[13] Thattaiparthasarathy KB, Pillay S, Ning H, Vaidya UK. Process simulation, design and manufacturing of a long fiber thermoplastic composite for mass transit application. Compos Appl Sci Manuf 2008;39(9):1512–21.
[14] Oliveira PR, May M, Panzera TH, Hiermaier S. Bio-based/green sandwich structures: a review. Thin-Walled Struct 2022;177:109426.
[15] Grünewald J, Parlevliet P, Altstädt V. Manufacturing of thermoplastic composite sandwich structures:A review of literature. J Thermoplast Compos Mater 2017;30(4):437–64.
[16] Davies JM. Lightweight sandwich construction. John Wiley & Sons; 2008.
[17] Karaduman Y, Onal L. Flexural behavior of commingled jute/polypropylene nonwoven fabric reinforced sandwich composites. Compos B Eng 2016;93:12–25.
[18] Kolahchi R, Zhu S-P, Keshtegar B, Trung N-T. Dynamic buckling optimization of laminated aircraft conical shells with hybrid nanocomposite martial. Aero Sci Technol 2020;98:105656.
[19] Keshtegar B, Farrokhian A, Kolahchi R, Trung N-T. Dynamic stability response of truncated nanocomposite conical shell with magnetostrictive face sheets utilizing higher order theory of sandwich panels. Eur J Mech Solid 2020;82:104010.
[20] Keshtegar B, Motezaker M, Kolahchi R, Trung N-T. Wave propagation and vibration responses in porous smart nanocomposite sandwich beam resting on Kerr foundation considering structural damping. Thin-Walled Struct 2020;154:106820.
[21] Motezaker M, Kolahchi R, Rajak DK, Mahmoud SR. Influences of fiber reinforced polymer layer on the dynamic deflection of concrete pipes containing nanoparticle subjected to earthquake load. Polym Compos 2021;42(8):4073–81.
[22] Kolahchi R, Keshtegar B, Trung N-T. Optimization of dynamic properties for laminated multiphase nanocomposite sandwich conical shell in thermal and magnetic conditions. J Sandw Struct Mater 2021;24(1):643–62.
[23] Al-Furjan MSH, Yang Y, Farrokhian A, Shen X, Kolahchi R, Rajak DK. Dynamic instability of nanocomposite piezoelectric-leptadenia pyrotechnica rheological elastomer-porous functionally graded materials micro viscoelastic beams at various strain gradient higher-order theories. Polym Compos 2022;43(1):282–98.
[24] Sargianis JJ, Kim H-I, Andres E, Suhr J. Sound and vibration damping characteristics in natural material based sandwich composites. Compos Struct 2013;96:538–44.
[25] Le Duigou A, Deux J-M, Davies P, Baley C. PLLA/flax mat/balsa bio-sandwich—environmental impact and simplified life cycle analysis. Appl Compos Mater 2012;19(3):363–78.
[26] Al-Furjan MSH, Shan L, Shen X, Kolahchi R, Rajak DK. Combination of FEM-DQM for nonlinear mechanics of porous GPL-reinforced sandwich nanoplates based on various theories. Thin-Walled Struct 2022;178:109495.
[27] Al-Furjan MSH, Shan L, Shen X, Zarei MS, Hajmohammad MH, Kolahchi R. A review on fabrication techniques and tensile properties of glass, carbon, and Kevlar fiber reinforced rolymer composites. J Mater Res Technol 2022;19:2930–59.
[28] Standard B. Fibre-reinforced plastic composites — determination of flexural properties. BS EN ISO 1998;14125. +A1:2011.
[29] Standard B. Plastics — determination of tensile properties — Part 4: test conditions for isotropic and orthotropic fibre-reinforced plastic composites. BS EN ISO 1997;527–4.
[30] Adusumali RB, Reifferscheid M, Weber H, Roeder T, Sixta H, Gindl W. Mechanical properties of regenerated cellulose fibres for composites. In: Macromolecular symposia. Wiley Online Library; 2006. p. 119–25.
[31] Timoshenko S. Strength of materials, Part I, elementary theory and problems. D. Van Nostrand Company; 1955.
[32] Carlsson LA, Kardomateas GA. Structural and failure mechanics of sandwich composites. Springer Science & Business Media; 2011.
[33] Birman V, Bert CW. On the choice of shear correction factor in sandwich structures. J Sandw Struct Mater 2002;4(1):83–95.
[34] Astm D:7250/D7250M - 06. Standard practice for determining sandwich beam flexural and shear stiffness. ASTM International.
[35] Du Y, Yan N, Kortschot MT. Light-weight honeycomb core sandwich panels containing biofiber-reinforced thermoset polymer composite skins: fabrication and evaluation. Compos B Eng 2012;43(7):2875–82.
[36] Li Y, Zhu J, Wei S, Ryu J, Sun L, Guo Z. Poly(propylene)/Graphene nanoplatelet nanocomposites: melt rheological behavior and thermal, electrical, and electronic properties. Macromol Chem Phys 2011;212(18):1951–9.
[37] Brandrup J, Immergut EH, Grulke EA, Abe A, Bloch DR. Polymer handbook. New York: Wiley; 1999.